

Synthesis and optical properties of Mn²⁺/Mn⁴⁺ doped ZnWO₄ powders for multi-purpose applications

Swagata Chakraborty^{©1,2}, Joydip Dutta^{©3}, Swarat Chaudhuri^{©2}, Mitesh Chakraborty^{©2,*}

Received 4 May 2025; Received in revised form 18 August 2025; Accepted 19 September 2025

Abstract

In the present investigation, pure $ZnWO_4$ and $1 \, mol\% \, Mn$ -doped $ZnWO_4$ ($ZnWO_4$: Mn^{2+} and $ZnWO_4$: Mn^{4+}) ceramic powders were synthesized by the conventional solid-state reaction method. The structural and microstructural studies were performed using X-ray diffraction, field emission scanning electron microscopy and Raman spectroscopy. The effect of peak shifts in XRD patterns on the lattice parameters is analysed in the prepared samples. Raman studies confirm the presence of Mn^{2+} and Mn^{4+} in the host matrix. The chromaticity parameters of the prepared samples are evaluated using a Commission Internationale de l'Elcairage (CIE) diagram. The study of the downconversion spectra of the prepared samples using an ultra-violet (UV) laser source suggests that transition metal-doped ceramics are a significant class of materials that can produce emissions for cool light-emitting diode applications.

Keywords: ZnWO₄, Mn-doping, structure, optical properties, photoluminescence

I. Introduction

It is well known that the tungstate-based oxide materials have immense applications in different electronic instruments viz. photoluminescence property for displays, light emitting diodes (LEDs), microwaves, optical communication, scintillation, dielectric resonators, capacitors, sensing activity, etc. [1,2]. These type of materials can be synthesized at high temperatures, shows novel features for commercial purposes because of high chemical stability and high absorption coefficient, One of these materials is zinc tungstate (ZnWO₄) which is intensively investigated [3,4]. ZnO, being one of the raw ingredients for the preparation of ZnWO₄, is selected as it has wide direct/indirect energy band gap. Hence by suitable selection of dopants, the properties of the host matrix can be explored for a particular electronic application [5]. From literature survey, it has been found that there are many different methods to prepare ZnWO₄ at the bulk/nano level.

*Corresponding author: +91 7631357351 e-mail: miiteshkchakraborty@gmail.com

In the present study, ZnWO₄ modified with 1 mol% MnO and 1 mol% MnO₂ were synthesized separately. A comparative study was done to investigate the structural parameters by X-ray diffraction and surface modification by Raman and photoluminescence spectroscopy.

II. Experimental

2.1. Synthesis

The ZnWO₄, ZnWO₄:Mn²⁺ and ZnWO₄:Mn⁴⁺ powders were prepared by solid state reaction method by using ZnO, WO₃, MnO and MnO₂ as the primary reacting materials. The host precursors ZnO and WO₃ were taken from Merck with 99% purity and MnO and MnO₂ were purchased from Sigma Aldrich with 99.9% purity. The synthesis process follows two-step method. Firstly, the ingredients were manually mixed using agate pestle and mortar for 2 h. The mixed samples were then heated in a muffle furnace at 200 °C for 2 h. After that, the materials were ground and kept in an electronic furnace at 1000 °C for 8 h. The annealed samples were again mixed for further structural and surface investigation.

¹University Department of Physics, Ranchi University, Ranchi-834008, Jharkhand, India

²Department of Physics, St. Xavier's College, Ranchi-834001, Ranchi University, Ranchi, Jharkhand, India

³Central Research Facility, Indian Institute of Technology (Indian School of Mines) Dhanbad-826004, Jharkhand, India

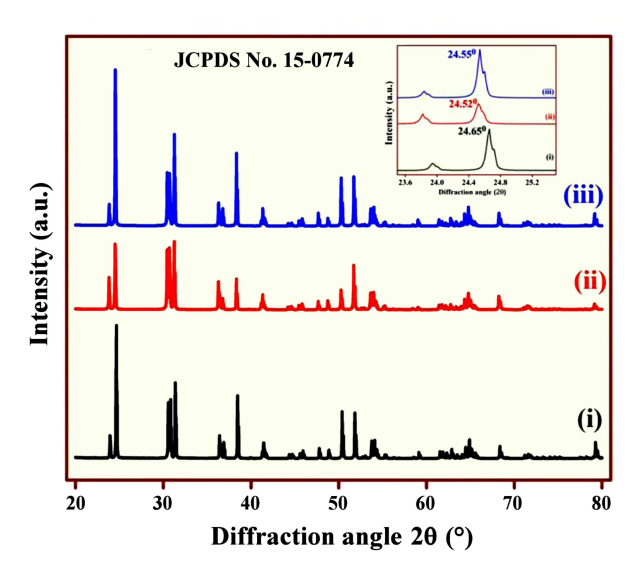


Figure 1. XRD diffraction patterns of the undoped $ZnWO_4$ (i), $ZnWO_4$: Mn^{2+} (ii) and $ZnWO_4$: Mn^{4+} (iii) samples (inset shows shift of themost intense peak)

2.2. Characterization techniques

X-ray diffraction (XRD) patterns of the prepared ceramics were recorded using Rigaku D/Max 2200 with Cu K α radiation with wavelength $\lambda=1.5406\,\text{Å}$ in the diffraction angle range of 10° to 80° at a scanning rate of $0.04\,^\circ$ /min. The photoluminescence emission spectra are recorded by using a Lifetime Spectrometer upon excitation with a Xenon arc lamp. Raman shift analysis was recorded by using Horiba Scientific (LabRAM HR-UV-Open) spectrometer. The vibrational analysis was done using the FTIR instrument from Perkin Elmer. All characterizations were performed at room temperature (~28 °C).

III. Results and discussion

3.1. XRD analysis

The structural investigation of the prepared ZnWO₄, ZnWO₄:Mn²⁺ and ZnWO₄:Mn⁴⁺ ceramic powders was performed using XRD (Fig. 1). The XRD patterns resemble monoclinic phase from JCPDS No. 15-0774 [3,6] and sharp peaks confirm good crystallinity of the prepared materials. The observed shift of XRD peaks (inset in Fig. 1) for the powders doped with Mn²⁺ and Mn⁴⁺ in comparison to the undoped sample confirms incorporation of Mn ions in ZnWO₄ structure. It is clearly visible from inset in Fig. 1 that the peak shifts towards the lower diffraction angle for the doped sample (ZnWO₄:Mn²⁺) as compared to the undoped sample. The reason is the smaller ionic radius of Zn²⁺ $(0.74 \,\text{Å})$ in comparison to that of Mn²⁺ $(0.84 \,\text{Å})$, which causes the increase of the unit cell volume, thereby decreasing d-spacing. It is also clear from Fig. 1 that the diffraction intensity first decreases with Mn²⁺ ion doping and again increases comparatively for Mn⁴⁺ ion. This could indicate that there is a change in the number of defects with incorporation of Mn²⁺ and Mn⁴⁺ ions in the host lattice. Another reason could also be the change in the surface-to-volume ratio, which modifies the surface thereby changing the crystallite size [7,8]. The crystallite size and micro strain calculated by using the Scherer formula of the prepared samples were 61.55 nm/0.0023 for ZnWO₄, 65.93 nm/0.0024 for ZnWO₄:Mn²⁺ and 59.14 nm/0.0019 for ZnWO₄:Mn⁴⁺ sample.

3.2. FESEM investigation

The surface morphology and particle size distribution in the prepared samples were investigated by us-

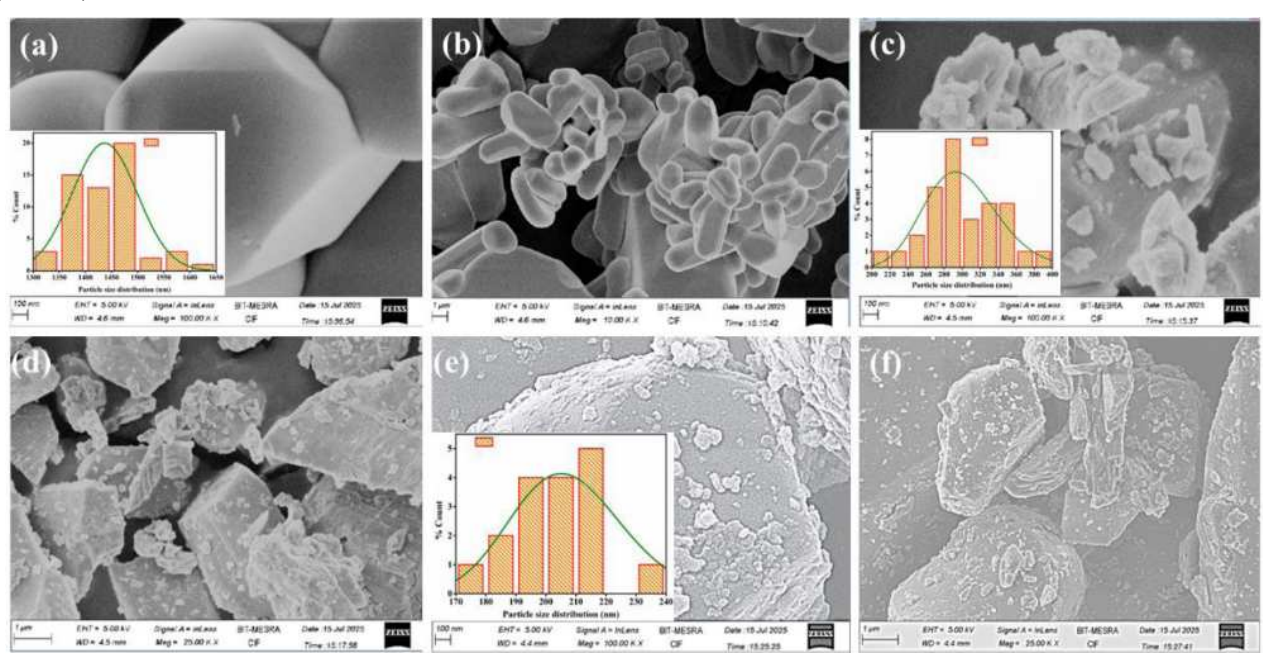


Figure 2. FESEM micrographs of undoped ZnWO₄ sample (a,b), ZnWO₄:Mn²⁺ (c,d) and ZnWO₄:Mn⁴⁺ (e,f) (insets show the corresponding particle size distribution)

ing field emission scanning electron microscopy (Fig. 2). The average particle sizes of these samples were evaluated using the ImageJ software, and they were 1476, 301 and 208 nm for the ZnWO₄, ZnWO₄:Mn²⁺ and ZnWO₄:Mn⁴⁺ powders, respectively. The micrographs reveal narrow particle size distribution. The particles appear to be of non-equal sides, which is consistent with the XRD patterns discussed in the previous section resembling monoclinic phase. It is evident from these micrographs that the particles are agglomerated and porous.

3.3. Raman investigation

The Raman spectra of the doped ceramics are shown in Fig. 3. It is clear that intensities of the characteristic Raman peaks are lower for the sample doped with Mn⁴⁺. This may be due to the decrease in the number of defects at the surface of the prepared host material. This is consistent with the XRD results discussed above.

The bands at around 88, 120, 191 and $340 \,\mathrm{cm}^{-1}$ are due to the acoustic phonon mode, E_{2L} , $2E_{2L}$ and E_{2H-2L} vibrational modes of ZnO, respectively [3,9]. Six peaks correspond to the stretching vibrations of the W-O bonds at around 405, 543, 676, 705, 782 and 905 cm⁻¹. These vibrations confirm the presence of WO₆ octahedra in the prepared samples [10]. The shoulders at around 311 and 513 cm⁻¹ may be related to the Mn induced zinc vacancy in the host. In addition to above mentioned characteristic bands observed in spectrum of the ZnWO₄:Mn²⁺ powder, there are a few peaks (555, 594, 637 and 974 cm⁻¹) characteristic for the spectrum of the ZnWO₄:Mn⁴⁺ powder (Fig. 4). The peaks at around 555 and 637 cm⁻¹ may be related to α -MnO₂ and β -MnO₂, respectively [11]. The shoulders at around 594 and 974 cm⁻¹ may be due to some intrinsic defects as the surface modified due to Mn⁴⁺ doping [12]. The additional oxygen ion may have changed the chemical bonding of Mn at the cationic site of Zn with the oxygen anions.

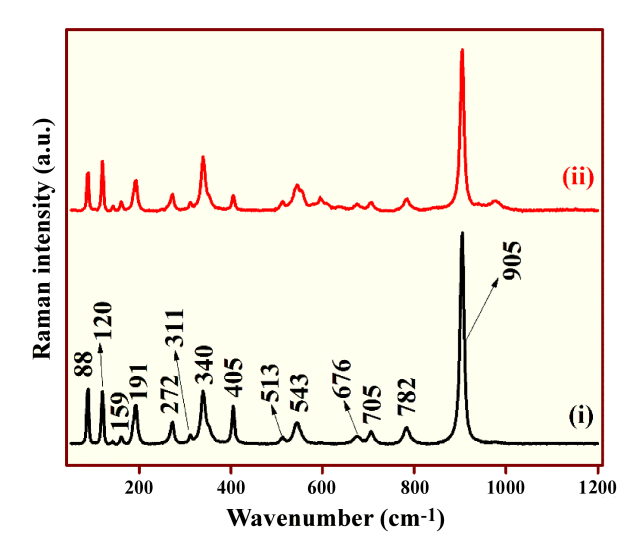


Figure 3. Raman spectra of the $ZnWO_4$: Mn^{2+} (i) and $ZnWO_4$: Mn^{4+} (ii)

3.4. Photoluminescence analysis

The photoluminescence (PL) emission spectra of the doped samples under 325 nm laser source excitation are presented in Fig. 4 in the wavelength range 300–800 nm. Both the samples exhibit three broad emission bands at around 377, 500 and 709 nm.

The emission bands of the $\rm Mn^{2+}$ doped sample at around 377 and 500 nm are related to $^2\rm A_1(^4\rm D) \rightarrow ^6\rm A_1(^6\rm S)$ and $^4\rm T_2(^4\rm G) \rightarrow ^6\rm A_1(^6\rm S)$, respectively [13]. For the $\rm ZnWO_4:Mn^{2+}$ material a sharp intense peak near 441 nm is also observed (Fig. 4) highlighted by a green rectangular region. This peak may be due to some interstitial vacancy due to substitution of larger $\rm Mn^{2+}$ ion (0.84 Å) at the $\rm Zn^{2+}$ site (0.74 Å) of the $\rm ZnWO_4$ structure [14].

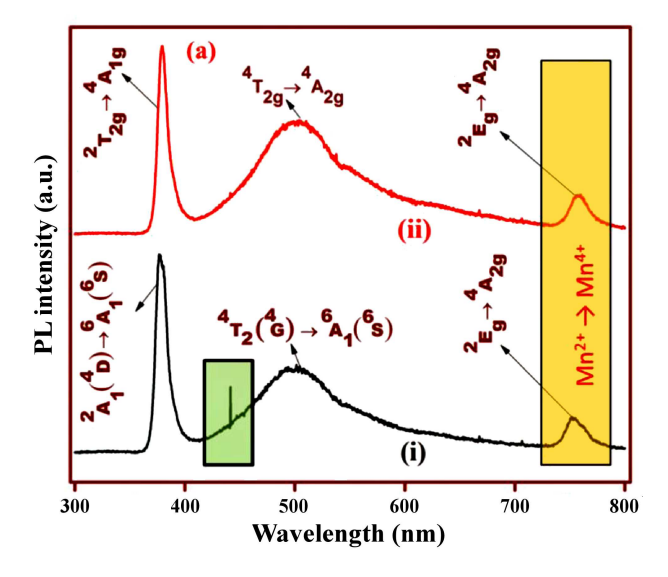


Figure 4. Photoluminescence spectra of the prepared samples ZnWO₄:Mn²⁺ (i) and ZnWO₄:Mn⁴⁺ (ii)

The peak near 441 nm is absent in the spectrum of the ZnWO₄:Mn⁴⁺ powder (Fig. 4). This may be due to the substitutional occupancy of smaller Mn⁴⁺ ion (0.61 Å) at the Zn^{2+} site (0.74 Å). Hence, incorporation of Mn^{4+} ion in the ZnWO₄ lattice may lead to some structural modification. This difference in behaviour between two doped samples could also be evidenced from optical images (not presented here). Thus, the optical image of the Mn⁴⁺ doped sample is comparatively more illuminated and sharp as compared to that of the Mn2+ doped powder. The broad PL emissions near 377 and 500 nm correspond to $2T_{2g} \rightarrow 4A_{1g}$ and $4T_{2g} \rightarrow 4A_{2g}$ energy levels of Mn⁴⁺ ion, respectively [15]. The wide band at around 500 nm may be due to the inhomogeneous broadening which is formed by phonon transitions. When the prepared sample is excited by 325 nm laser source, the electron first moves to some excited state and then to the lower energy state either by non-radiative recombination and/or emission of suitable wavelengths. These processes are induced by the crystalline defects present in the material [16]. We have also observed a broad band around 709 nm in both spectra (Fig. 4) as presented by

orange highlighter. This is related to $2E_g \rightarrow 4A_{2g}$ energy transitions of Mn⁴⁺ [17]. The observation of the same band in the spectrum of Mn²⁺ doped sample may be due to the transition of some Mn²⁺ ions to Mn⁴⁺ when exposed to laser source and formation of oxygen vacancies, as the compound is formed at a high temperature of about 1000 °C [3,12].

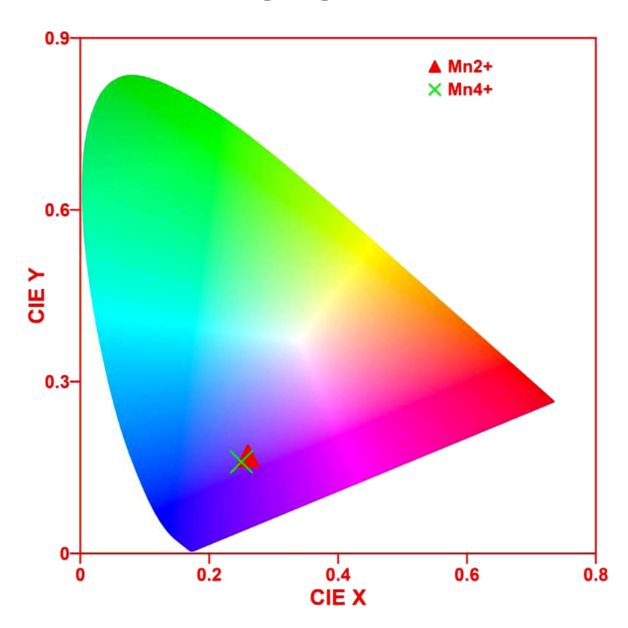


Figure 5. CIE plot of Mn²⁺ and Mn⁴⁺ doped ZnWO₄

3.5. Photometric investigation

The Commission Internationale L'Eclairage (CIE) colour coordinate software was used to examine the distribution of luminescent intensity of the prepared ceramic powders [18]. The CIE colour coordinates for the downconversion emission intensity of the prepared samples are shown in Fig. 5. From the CIE plot, it is clear that the CIE coordinates are present in the blue region. The ZnWO₄:Mn²⁺ sample is labelled with a red triangle mark having coordinates (0.26, 0.17) and the ZnWO₄:Mn⁴⁺ sample is represented with a green cross mark with coordinates (0.25, 0.16). The colour purity (*CP*) and colour correlated temperature (*CCT*) of the prepared samples was calculated using the following equations [19,20]:

$$CP = \sqrt{\frac{(X_e - X_i)^2 + (Y_e - Y_i)^2}{(X_0 - X_i)^2 + (Y_0 - Y_i)^2}} \times 100\%$$
 (1)

$$CCT = -499n^3 + 3525n^2 - 6823.3n + 5520.33$$
 (2)

where (X_e, Y_e) , (X_i, Y_i) and (X_0, Y_0) are the CIE coordinates of the prepared samples, the standard light source (i.e. white light where $X_i = 0.33$ and $Y_i = 0.33$) and the dominant wavelength of the respective colours. In addition, $n = (X_e - X_E)/(Y_e - Y_E)$ and (X_E, Y_E) are the coordinates of CCT epicentre; the standard values are taken to be (0.332, 0.186). The photometric parameters are reported in Table 1.

Table 1. The CIE coordinates and the calculated colour purity (CP) and colour correlated temperature (CCT) of the prepared samples

	X_e	Y_e	X_0	Y_0	<i>CP</i> [%]	CCT [K]
ZnWO ₄ :Mn ²⁺	0.26	0.17	0.21	0.041	55.77	7677
ZnWO ₄ :Mn ⁴⁺	0.25	0.16	0.19	0.040	58.34	6056

From the calculated CCT values it is suggested that the prepared samples may be explored to design ultra daylight fluorescent cool LEDs used in manufacturing and specific workshops [21].

3.6. Thin film demonstration

Thin film containing the Mn⁴⁺ doped powder was prepared to demonstrate potential applications of the synthesized powders. For the thin film preparation, 30 mg of ZnWO₄:Mn⁴⁺ was dispersed in 15 ml ethanol using a sonicator (ultrasonic probe) at 50 kHz frequency for 3 h. In the formed homogenous dispersion aminopropyl tri-ethoxy silane (APTES) was added using a dropper and simultaneous stirring at 400 rpm, at 60 °C for 3 h. The obtained solution was deposited on a glass plate by spin-coating. Under UV light exposure, the blue emission of the sample is clearly visible by naked eye as shown in Fig. 6. This shows that the prepared sample may be applied as security ink, and in thin-film photovoltaics, thin-film batteries, decorative and optical coatings, etc. [22,23].

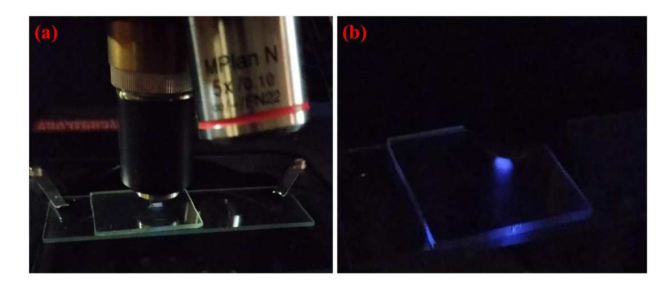


Figure 6. CIE plot of Mn²⁺ and Mn⁴⁺ doped ZnWO₄

IV. Conclusions

ZnWO₄:Mn²⁺ and ZnWO₄:Mn⁴⁺ ceramic powders were synthesized by conventional solid state reaction method. The presence of monoclinic ZnWO₄ phase was confirmed by XRD and it was also observed that the crystallinity of the powders increases with decrease in ionic radius of the manganese cation substituted at the Zn site. The FESEM micrographs reveal irregular shaped structures of the prepared samples. The histogram analysis shows narrow particle size distribution of the prepared ceramics. The Raman spectra show the existence of different vibrational modes of Zn–O and W–O in the host material. Some characteristic Raman peaks also show the presence of α and β phases of MnO₂. A comparative surface analysis on Mn²⁺ and Mn⁴⁺ doped ZnWO₄ host is reported in the present

study. The evidence of oxygen vacancies is affirmed through Raman and photoluminescence studies. The prepared samples may be used to prepare cool LEDs, thin-film applications, etc.

Acknowledgement: The authors are grateful to Central Instrumentation Facility, I.I.T. (I.S.M.) Dhanbad, Jharkhand, India for providing instrumental facilities. One of the authors, Dr Mitesh Chakraborty also appreciates the University Grants Commission (UGC), New Delhi, India for providing financial assistance in the form of Colleges with Potential for Excellence (CPE) status to St. Xavier's College, Ranchi, India (DO/21-49/2014/PE).

References

- G.B. Kumar, K. Sivaiah, S. Buddhudu, "Synthesis and characterization of ZnWO₄ ceramic powder", *Ceram. Int.*, 36 (2010) 199–202.
- E. Sani, A. Brugioni, L. Mercatelli, D. Parisi, E.V. Zharikov, D. Lis, K.A. Subbotin, "Yb-doped double tungstates for down-conversion applications", *Opt. Mater.*, 94 (2019) 415–422.
- S. Chakraborty, J. Dutta, M. Chakraborty, V. Mishra, "Structural and photoluminescence investigation of Gd³⁺ doped ZnWO₄ phosphor for cyan emitting lighting applications", AIP Conf. Proc., 3196 (2024) 050002.
- S. Chakraborty, J. Dutta, M. Chakraborty, "Enriched upconversion emission and electrical properties of Er³⁺/Yb³⁺/Mn: ZnWO₄ phosphors for display and anticounterfeit applications", *Mater. Sci. Semiconduc. Process.*, 192 (2025) 109404–109413.
- M. Chakraborty, D. Banerjee, S. Singh, J. Dutta, "Photoluminescence and EPR investigation in ZnO: Gd³⁺, Yb³⁺ phosphors for application in light emitting diode", *Mater. Sci. Semiconduc. Process.*, **166** (2023) 107758.
- M.I. Osotsi, D.K. Macharia, B. Zhu, Z. Wang, X. Shen, Z. Liu, L. Zhang, Z. Chen, "Synthesis of ZnWO_{4-x} nanorods with oxygen vacancy for efficient photocatalytic degradation of tetracycline", *Prog. Nat. Sci. Mater. Int.*, 28 (2018) 408-415
- R. Perrella, D.P. Santos, G. Poirier, M. Goes, S.J. Ribeiro, M. A. Schiavon, J.L. Ferrari, "Er³⁺ doped Y₂O₃ obtained by polymeric precursor: Synthesis, structure and upconversion emission properties", *J. Lumin.*, **149** (2014) 333– 340.
- 8. C-Y. Yang, S. Som, S. Das, C-H. Lu, "Synthesis of Sr₂Si₅N₈:Ce³⁺ phosphors for white LEDs via an efficient chemical deposition", *Sci. Rep.*, **7** (2017) 45832.
- 9. H.-W. Shim, I.-S. Cho, K.S. Hong, A.-H. Lim, D.-W. Kim, "Wolframite-type ZnWO₄ nanorods as new anodes for Li-ion batteries", *J. Phys. Chem. C*, **115** (2011) 16228–16233.

- M-T. Liu, E-C. Xiao, J-Q. Lv, Z-M. Qi, Z. Yue, Y. Chen, G. Chen, F. Shi, "Phonon characteristics and intrinsic properties of single phase ZnWO₄ ceramic", *J. Mater. Sci. Mater. Electon.*, 31 (2020) 6192–6198.
- 11. V. Sannasi, K. Subbian, "Influence of Moringa oleifera gum on two polymorphs synthesis of MnO₂ and evaluation of the pseudo-capacitance activity", *J. Mater. Sci. Mater. Electron.*, **31** (2020) 17120–17132.
- C. Julien, M. Massot, R. Baddour-Hadjean, S. Franger, S. Bach, J.P. Pereira-Ramos, "Raman spectra of birnessite manganese dioxides", *Solid State Ionics*, **159** (2003) 345– 356
- M.H. Wan, P.S. Wong, R. Hussin, H.O. Lintang, "Physical and optical properties of calcium zinc borophosphate glasses doped with manganese ions", *Spectrosc. Lett.*, 48 (2015) 473–480.
- 14. S. Tang, J. Su, T. Lu, Y. Ma, J. Ke, J. Zhang, T. Lu, Z. Song, H. Liu, "A thick overgrowth of CVD synthetic diamond on a natural diamond", *J. Gemmol.*, **36** (2018) 134–141.
- 15. J.Y. Park, J.S. Joo, H.K. Yang, M. Kwak, "Deep redemitting Ca₁₄Al₁₀Zn₆O₃₅: Mn⁴⁺ phosphors for WLED applications", *J. Alloys Compd.*, **714** (2017) 390–396.
- R.N. Bhargava, D. Gallagher, X. Hong, A. Numikko, "Optical properties of manganese-doped nanocrystalsfor ZnS", *Phys. Rev. Lett.*, 72 (1994) 416.
- 17. K. Li, R.V. Deun, "Enhancing the energy transfer from Mn⁴⁺ to Yb³⁺ via a Nd³⁺ bridge role in Ca₃La₂W₂O₁₂: Mn⁴⁺, Nd³⁺,Yb³⁺ phosphors for spectral conversion of c-Si solar cells", *Dyes Pigments*, **162** (2019) 990–997.
- 18. R.S. Yadav, S.B. Rai, "Surface analysis and enhancement photoluminescence via Bi³⁺ doping in a Tb³⁺ doped Y₂O₃ nano-phosphor under UV excitation", *J. Alloys Compd.*, **700** (2017) 228–237.
- 19. Y. Wang, B. Deng, Y. Ke, S. Shu, R. Liu, R. Yu, "Spectroscopic investigation of La₇Ta₃W₄O₃₀: Sm³⁺ orange-red phosphors for white LEDs", *Arab. J. Chem.*, **13** (2020) 5581–5592.
- R. Prasad, M. Prasad, J. Dutta, M. Chakraborty, "Tailoring Er³⁺ doped ZnTiO₃ ceramic surfaces for high color purity green emitting display device applications", *Surf. Eng.*, 41 [3] (2025) 438–442.
- S. Zhang, Z. Hao, L. Zhang, G-H. Pan, W. Huajun, X. Zhang, Y. Luo, L. Zhang, H. Zhao, J. Zhang, "Efficient-blue emitting phosphor SrLu₂O₄: Ce³⁺ with high thermal stability for near ultraviolet (~400 nm) LED-chip based white LEDs", Sci. Rep., 8 (2018) 10463–10471.
- 22. Y. Ding, C. Wang, L. Pei, Q. Mao, S. Bandaru, R. Zheng, S. Maitra, M. Liu, L-H. Chen, B-L. Su, J. Zhong, "Mn⁴⁺ activated phosphors in photoelectric and energy conversion devices", *J. Ener. Chem.*, **86** (2023) 277–299.
- 23. J. Dutta, M. Chakraborty, V.K. Rai, "Tm³⁺, Yb³⁺: Zn₂TiO₄ near infrared to blue upconversion phosphors for anti-counterfeit applications", *RSC Adv.*, **13** (2023) 23386–23395.